Robust H_∞ Control Design for the Space Station with Structured Parameter Uncertainty

Kuk-Whan Byun* and Bong Wie†
Arizona State University
Tempe, Arizona

David Geller‡ and John Sunkel§
NASA Johnson Space Center
Houston, Texas

Abstract

A robust H_∞ control design methodology and its application to a Space Station attitude and momentum control problem are presented. This new approach incorporates nonlinear multi-parameter variations in the state-space formulation of H_∞ control theory. An application of this robust H_∞ control synthesis technique to the Space Station control problem yields a remarkable result in stability robustness with respect to the moments-of-inertia variation of about 73% in one of the structured uncertainty directions. The performance and stability of this new robust H_∞ controller for the Space Station are compared to those of other controllers designed using a standard linear-quadratic-regulator synthesis technique.

1. Introduction

The Space Station Freedom will employ control moment gyros (CMGs) as primary actuating devices during normal flight mode operation, and it will utilize the gravity-gradient torque for the CMG momentum management [1,2]. An attitude determination system of the Space Station will employ rate gyros and star trackers to compute the states of the vehicle for control purposes. Multivariable, periodic-disturbance accommodating controllers have been developed and are being considered for actual implementation to the Space Station Freedom [3–7].

As illustrated in Fig. 1, the Space Station will be assembled and maintained using the Mobile Remote Manipulator System (MRMS) and its Mobile Transporter (MT). The MRMS/MT carrying a large payload will cause significant changes in the inertia property of the Space Station; consequently, it will affect the overall performance and stability of the control system. Study results on the effects of such MRMS/MT operations (e.g., a "bay" translation along the pitch axis and 180-deg slew maneuver about the pitch axis) can be found in [7]. The study results of [7] indicate that some form of adaptive or robust control with more than 50% inertia variation margins is necessary to account for the large changes in the inertia property caused by the motion of the MRMS/MT and its large payload. The study results also indicate that a high-bandwidth controller has unacceptable transient responses during the payload maneuvers.

In this paper, a robust control synthesis technique based on H_∞ control theory is developed and applied to the robust control design problem of the Space Station discussed above. This new approach incorporates nonlinear multi-parameter variations in the state-space formulation of H_∞ control theory [8-10]. An application of this robust H_∞ control synthesis technique to the Space Station yields a remarkable result in stability robustness with respect to the moments-of-inertia variation of about 73% in one of the structured uncertainty directions. Such a 73% inertia variation margin is rather significant compared to the margin of 44% of a typical linear-quadratic-regulator (LQR) design [3-7] with nearly the same control bandwidth as the robust H_∞ controller.

This paper is organized as follows. In Section 2 a robust full-state feedback control synthesis technique based on the H_∞ control theory is presented, which exploits the concept of input-output decomposition of the uncertain system parameters [10-13]. A "full-state" feedback control is considered since the full states of the vehicle are available from an attitude determination system of the Space Station. A similar approach for the dynamic compensator design can be found in [13]. The linearized equations of motion of the Space Station are reviewed in Section 3. A robust H_∞ controller is synthesized in Section 4, with special emphasis on the input-output decomposition of nonlinear, uncertain multi-parameters of the system.

*Currently, Research Scientist at Dynacs Engineering Co., Inc., Clearwater, Florida.
†Associate Professor, Dept. of Mechanical and Aerospace Engineering, Member AIAA.
‡Aerospace Engineer, Mission Planning and Analysis Division, Member AIAA.
§Aerospace Engineer, Avionics Division, Member AIAA.

2. Robust H_∞ Control Synthesis

Background

In recent years there has been a growing interest in robust stabilization and control based on H_∞ control theory [8-10,13-15], and substantial contributions have already been made to the state-space characterization of the H_∞ control problems [8,9]. Most standard H_∞-related control techniques are, however, concerned with the sensitivity minimization with respect to the external disturbances, and are not directly related to the structured parameter uncertainty. Recently, a new way of incorporating parameter uncertainty in the robust H_∞ compensator design is developed in [10,13] by converting the parameter-insensitive control problem into a conventional H_∞ problem. The state-space solution to a standard H_∞ control problem in [8,9] is then utilized by redefining the structured parameter variations in terms of a fictitious input and output.

In this section, such a robust H_∞ control synthesis technique developed in [10,13] is reviewed with special emphasis on the new concept of "directional" parameterization of nonlinear, uncertain parameters. Only the "full-state" feedback control case is considered here since the Space Station control problem does not need the consideration of state estimation. A more general case with dynamic compensation can be found in [10,13].

The H_∞ space consists of functions which are bounded and stable. The H_∞-norm of a real-rational matrix $\boldsymbol{T}(s)$ is defined as

$$\begin{aligned} \|T\|_\infty &\triangleq \sup\{\,\|\boldsymbol{T}(s)\| : \mathrm{Re}(s) > 0\} \\ &= \sup_\omega \|\boldsymbol{T}(j\omega)\| \\ &= \sup_\omega \bar{\sigma}[\boldsymbol{T}(j\omega)] \end{aligned}$$

where $\bar{\sigma}[\boldsymbol{T}(j\omega)]$ denotes the largest singular value of $\boldsymbol{T}(j\omega)$ for a given ω.

In this paper, we consider a linear, time-invariant multivariable system described by [8,9]

$$\dot{\boldsymbol{x}}(t) = \boldsymbol{A}\,\boldsymbol{x}(t) + \boldsymbol{B}_1\,\boldsymbol{w}(t) + \boldsymbol{B}_2\,\boldsymbol{u}(t) \qquad \text{(1a)}$$

$$\boldsymbol{z}(t) = \boldsymbol{C}_1\boldsymbol{x}(t) + \boldsymbol{D}_{11}\boldsymbol{w}(t) + \boldsymbol{D}_{12}\boldsymbol{u}(t) \qquad \text{(1b)}$$

where $\boldsymbol{x}(t)$ is an n-dimensional state vector and is assumed to be directly measured, $\boldsymbol{w}(t)$ an m_1-dimensional disturbance vector, $\boldsymbol{u}(t)$ an m_2-dimensional control vector, and $\boldsymbol{z}(t)$ a p_1-dimensional controlled output vector.

The transfer function representation of this system is given by

$$\boldsymbol{z}(s) = \begin{bmatrix} \boldsymbol{P}_{11}(s) & \boldsymbol{P}_{12}(s) \end{bmatrix} \begin{bmatrix} \boldsymbol{w}(s) \\ \boldsymbol{u}(s) \end{bmatrix} \qquad (2)$$

while the plant transfer matrix $\boldsymbol{P}(s)$ is related to the matrices in Eqs. (1) by

$$\boldsymbol{P}(s) = \boldsymbol{C}_1(s\boldsymbol{I} - \boldsymbol{A})^{-1}\begin{bmatrix} \boldsymbol{B}_1 & \boldsymbol{B}_2 \end{bmatrix} + \begin{bmatrix} \boldsymbol{D}_{11} & \boldsymbol{D}_{12} \end{bmatrix} \qquad (3)$$

Internal Feedback Loop

Consider an uncertain dynamical system described as

$$\begin{bmatrix} \dot{\boldsymbol{x}} \\ \boldsymbol{z} \end{bmatrix} = \begin{bmatrix} \hat{\boldsymbol{A}} & \hat{\boldsymbol{B}}_1 & \hat{\boldsymbol{B}}_2 \\ \boldsymbol{C}_1 & \boldsymbol{D}_{11} & \boldsymbol{D}_{12} \end{bmatrix} \begin{bmatrix} \boldsymbol{x} \\ \boldsymbol{w} \\ \boldsymbol{u} \end{bmatrix} \qquad (4)$$

where $\boldsymbol{C}_1$, $\boldsymbol{D}_{11}$, and $\boldsymbol{D}_{12}$ are not subject to parameter variations. The system matrices possessing uncertain parameters in Eq. (4) are linearly decomposed into an internal feedback loop [11,12,13] as follows:

$$\begin{bmatrix} \dot{\boldsymbol{x}} \\ \boldsymbol{z} \end{bmatrix} = \left\{ \begin{bmatrix} \boldsymbol{A} & \boldsymbol{B}_1 & \boldsymbol{B}_2 \\ \boldsymbol{C}_1 & \boldsymbol{D}_{11} & \boldsymbol{D}_{12} \end{bmatrix} + \Delta_e \right\} \begin{bmatrix} \boldsymbol{x} \\ \boldsymbol{w} \\ \boldsymbol{u} \end{bmatrix} \qquad (5)$$

where the first matrix in the right-hand side is the nominal system matrix and Δ_e is the perturbation matrix defined as

$$\Delta_e \triangleq \begin{bmatrix} \Delta\boldsymbol{A} & \Delta\boldsymbol{B}_1 & \Delta\boldsymbol{B}_2 \\ \boldsymbol{0} & \boldsymbol{0} & \boldsymbol{0} \end{bmatrix} \qquad (6)$$

Suppose that there are l independent parameters $p_1, \cdots, p_l$ and that their variations are bounded as $p_i \le p_i \le \bar{p}_i$, or $|\Delta p_i| \le 1$. If Δ_e is linearly dependent of each uncertain parameter, then it can be decomposed as derived in [11,13]. However, Δ_e may contain elements that are nonlinear combinations of Δp_i's. Variations in the uncertain matrix elements, Δe_i, are represented in a functional form as

$$\Delta e_i = \Delta e_i(\Delta \boldsymbol{p}) \quad \text{for } i = 1, \cdots, q$$

where $\Delta \boldsymbol{p} = [\Delta p_1, \cdots, \Delta p_l]^T$ and q is the number of the uncertain matrix elements of Δ_e. The perturbation matrix Δ_e is then decomposed as

$$\Delta_e = -\begin{bmatrix} \boldsymbol{M}_x \\ \boldsymbol{0} \end{bmatrix} \boldsymbol{E} \begin{bmatrix} \boldsymbol{N}_x & \boldsymbol{N}_w & \boldsymbol{N}_u \end{bmatrix} = -\boldsymbol{MEN} \qquad (7)$$

where the columns of $\boldsymbol{M}$ and the rows of $\boldsymbol{N}$ span the columns and the rows of Δ_e, respectively; and

$$\boldsymbol{E} = \begin{bmatrix} \Delta e_1(\Delta \boldsymbol{p}) & & \boldsymbol{0} \\ & \ddots & \\ \boldsymbol{0} & & \Delta e_q(\Delta \boldsymbol{p}) \end{bmatrix}. \qquad (8)$$

If Δe_i's are linear in Δp_i's, then the above input-output decomposition can be rearranged to become a rank-one input-output decomposition, which has been applied to a real-parameter variation problem [13].

Define the following new variables

$$\boldsymbol{x}_p \triangleq \begin{bmatrix} \boldsymbol{N}_x & \boldsymbol{0} & \boldsymbol{N}_w & \boldsymbol{N}_u \end{bmatrix} \begin{bmatrix} \boldsymbol{x} \\ \boldsymbol{w}_p \\ \boldsymbol{w} \\ \boldsymbol{u} \end{bmatrix}, \qquad \text{(9a)}$$

$$\boldsymbol{w}_p \triangleq -\boldsymbol{E}\,\boldsymbol{x}_p\,, \qquad \text{(9b)}$$

then the perturbed system, Eq. (5), and the input-output decomposition, Eq. (7), can be combined as:

$$\begin{bmatrix} \dot{x} \\ z_p \\ z \end{bmatrix} = \begin{bmatrix} A & M_x & B_1 & B_2 \\ N_x & 0 & N_w & N_u \\ C_1 & 0 & D_{11} & D_{12} \end{bmatrix} \begin{bmatrix} x \\ w_p \\ w \\ u \end{bmatrix} \quad (10a)$$

$$w_p = -E z_p \quad (10b)$$

where w_p and z_p are considered as the fictitious input and output, respectively, caused by the plant perturbation; and E is considered as a fictitious, internal feedback loop gain matrix.

The above internal feedback loop representation of the plant parameter uncertainty becomes useful for stability/performance robustness analysis discussed later in this section. In fact, the parameter-insensitive control synthesis problem becomes a convensional H_∞ disturbance attenuation problem, which can be easily solved by using the state-space formulation of the H_∞ control theory.

Directional Parameter Variations

A "hypercube" in the space of the plant parameters, centered at a nominal point, is often used as a stability robustness measure [16]. The robust control synthesis problem is then to find a controller which yields the largest hypercube that will fit within the existing, but unknown, region of stability in the plant's parameter space. In [16], a computational method is developed, which exploits the mapping theorem and the "multilinear" property of the plant's uncertain parameters. However, as shown later in this paper, the Space Station has the uncertain moments of inertia which appear in the internal feedback loop gain E as nonlinear functions.

One way to overcome the presence of such uncertain parameters in the internal feedback loop modeling is to consider $e_1, \cdots, e_q$ of E as new independent parameters and to find the worst possible bounds $\underline{e}_i$ and $\bar{e}_i$ for each e_i; that is, $\underline{e}_i \le e_i \le \bar{e}_i$. This approach then reduces to the standard input-output decomposition problem with q independent parameters. However, e_i's may be functionally dependent to each other through actual parameter variations, Δp_i's. Whenever e_i's are closely related, this approach will result in a very conservative control design; furthermore, some valuable information on the structured parameter variations is not utilized in this approach.

In order to exploite some structured or directional information on the plant parameter variations, the internal feedback loop gain matrix E is linearized about the nominal parameter set with respect to small Δp_i's as follows:

$$E \cong M_1 E_1 N_1 \quad (11a)$$

$$\Delta_e \cong -M M_1 E_1 N_1 N \quad (11b)$$

where E_1 contains only the actual, independent uncertain parameters. The standard form of an input-output decomposition such as Eq. (7), is obtained by re-defining M, N, and E as

$$\begin{aligned} M &\leftarrow M M_1 \\ N &\leftarrow N_1 N \\ E &\leftarrow E_1 \end{aligned} \quad (12)$$

In some cases, the plant parameter perturbations Δp_i's may possess a certain *directional* relationship with the following form:

$$\Delta p_i = g_i \delta \qquad \text{for } i = 1, \cdots, l \quad (13)$$

where g_i represents the direction and magnitude of Δp_i and δ is a scalar variable which represents the system uncertainty. Parameter variations involving a single parameter variable are referred to as *uni-directional* parameter variations, while those involving more than one parameter variable are referred to as *multi-directional* parameter variations.

The multi-directional parameter variations are characterized as:

$$\Delta p_i = g_{ij} \delta_j \quad \text{for } i = 1, \cdots, l \text{ and } j = 1, \cdots, r \quad (14)$$

where g_{ij} represents the direction and magnitude of Δp_i caused by δ_j for multi-directional perturbations.

For such cases with multi-directional parameter variations, the internal feedback loop gain E in Eq. (8) becomes a function of δ_j's:

$$E = \begin{bmatrix} \Delta e_1(\delta) & & 0 \\ & \ddots & \\ 0 & & \Delta e_q(\delta) \end{bmatrix} \quad (15)$$

where $\delta = [\delta_1, \cdots, \delta_r]^T$. Since E is nonlinear in δ_j's in general, the linearized input-output decomposition is again applied here, as in Eqs. (11) and (12), to be incorporated in the robust control synthesis.

Stability/Performance Robustness

A robust H_∞ full-state feedback control synthesis technique presented in this section exploits the internal feedback loop modeling concept and the H_∞ control theory. This new robust control design methodology is summarized in terms of three theorems. Detailed proofs of these theorems can be found in [8–10]. Development and application of robust H_∞ compensator synthesis can be found in [13].

The parameter uncertainty model given by Eq. (7) and the nominal plant described by Eq. (2) can be combined as

$$\begin{bmatrix} z_p \\ z \\ x \end{bmatrix} = \begin{bmatrix} G_{11} & G_{12} & G_{13} \\ G_{21} & G_{22} & G_{23} \\ G_{31} & G_{32} & G_{33} \end{bmatrix} \begin{bmatrix} w_p \\ w \\ u \end{bmatrix} \quad (16a)$$

$$w_p = -E z_p \quad (16b)$$

$$u = -K x \quad (16c)$$

where w_p and z_p are, respectively, the fictitious input and output, E is the fictitious internal loop gain matrix, and K is a full-state gain matrix to be determined.

The closed-loop system, but with the fictitious internal loop open, becomes:

$$\begin{bmatrix} z_p \\ z \end{bmatrix} = T \begin{bmatrix} w_p \\ w \end{bmatrix} \tag{17a}$$

$$w_p = -Ez_p \tag{17b}$$

where

$$T = \begin{bmatrix} T_{11} & T_{12} \\ T_{21} & T_{22} \end{bmatrix} \tag{18a}$$

$$T_{11} = G_{11} - G_{13}K(I + G_{33}K)^{-1}G_{31} \tag{18b}$$

$$T_{12} = G_{12} - G_{13}K(I + G_{33}K)^{-1}G_{32} \tag{18c}$$

$$T_{21} = G_{21} - G_{23}K(I + G_{33}K)^{-1}G_{31} \tag{18d}$$

$$T_{22} = G_{22} - G_{23}K(I + G_{33}K)^{-1}G_{32} \tag{18e}$$

The actual closed-loop transfer function matrix from w to z with plant perturbations becomes

$$T_{zw} = T_{22} - T_{21}E(I + T_{11}E)^{-1}T_{12} \tag{19}$$

Note that, in Eqs. (16) and (17), the parameter uncertainty does not appear in the transfer function matrices. Equations (17) can be used for the stability/performance robustness characterization. Sufficient conditions for robust stability and performance are provided by the following Theorems 1 and 2.

Theorem 1 (Stability Robustness)
$T_{zw}(s, \alpha E)$ $\forall \alpha \in [0,1]$ is robustly stable for $\|E\| \leq \epsilon$, and $\epsilon > 0$, if

$$\|T_{11}(s)\|_\infty < \epsilon^{-1}$$

where ϵ is a measure of the magnitude of the plant parameter uncertainty E in Eq. (8).

It is seen that T_{11} determines the stability robustness with respect to parameter uncertainty. Small $\|T_{11}\|_\infty$ allows large parameter variations for closed-loop stability. For this reason T_{11} is often referred to as robustness function [12]. The above theorem provides a sufficient condition for the closed-loop stability, resulting in a conservative control design. Since the condition in Theorem 1 is concerned with a deterministic bound, the H_∞ control theory can be employed for the internal feedback loop model. The next theorem provides a sufficient condition for guaranteed performance robustness.

Theorem 2 (Performance Robustness)
$T_{zw}(s, \alpha E)$ $\forall \alpha \in [0,1]$ is stable, and $\|T_{zw}(s, \alpha E)\|_\infty < \gamma$ $\forall \alpha \in [0,1]$ with $\|E\| \leq \gamma^{-1}$, if

$$\|T\|_\infty < \gamma \tag{20}$$

where T and T_{zw} are defined in Eqs. (17) and (19), and γ is an upper bound for the desired performance specification.

The above two theorems provide conditions for robust stability and performance of the perturbed closed-loop system in terms of T_{11} and T in Eqs. (17) and (18). The following re-definition of z, w, and the associated matrices enables us to employ the standard state-space representation given by Eq. (1):

$$z \leftarrow \begin{bmatrix} z_p \\ z \end{bmatrix}, \qquad w \leftarrow \begin{bmatrix} w_p \\ w \end{bmatrix},$$

$$B_1 \leftarrow \begin{bmatrix} M_x & B_1 \end{bmatrix}, \qquad C_1 \leftarrow \begin{bmatrix} N_x \\ C_1 \end{bmatrix}, \tag{21}$$

$$D_{11} \leftarrow \begin{bmatrix} 0 & N_w \\ 0 & D_{11} \end{bmatrix}, \qquad D_{12} \leftarrow \begin{bmatrix} N_u \\ D_{12} \end{bmatrix}.$$

The following theorem [8] gives a robust H_∞ controller which satisfies the condition in Eq. (20).

Theorem 3 (H_∞ Full-State Feedback Controller)
Assume that
(i) (A, B_2) is stabilizable and (C_1, A) is detectable,
(ii) $D_{12}^T \begin{bmatrix} C_1 & D_{12} \end{bmatrix} = \begin{bmatrix} 0 & I \end{bmatrix}$,
(iii) the rank of $P_{12}(j\omega)$ is m_2 for all ω, and
(iv) $D_{11} = 0$.
Given the above assumptions (i) through (iv), there exists an internally stabilizing controller such that, for the closed-loop transfer matrix T in Eqs. (17) and for a given design variable γ,

$$\|T\|_\infty < \gamma$$

if and only if the following Riccati equations

$$0 = A^T X + XA - X(B_2 B_2^T - \frac{1}{\gamma^2} B_1 B_1^T)X + C_1^T C_1 \tag{22}$$

have unique symmetric positive semi-definite solution X such that

$$A - (B_2 B_2^T - \frac{1}{\gamma^2} B_1 B_1^T)X \text{ and } A - B_2 B_2^T X \text{ are stable.}$$

A state-feedback gain that satisfies $\|T_{zw}\|_\infty < \gamma$, where γ is a design variable specifying an upper bound of the perturbed closed-loop performance T_{zw}, is then obtained as

$$K = B_2^T X \tag{23}$$

In order to achieve the desired closed-loop performance over all frequencies, T_{zw} is often formulated to include frequency-dependent weighting matrices. (A proper selection of the weighting matrices is an important step in any optimization-based design techniques, such as the linear-quadratic-gaussian (LQG) control and H_∞-optimization.) In this paper, constant diagonal weighting matrices are used. Inverses of the diagonal elements of the weighting matrix is referred to as weigthing factors. The weighting factors and γ represent relative input-output levels and overall closed-loop performance level, respectively. In the Appendix, the usage

of constant weightings, scaling, and orthogonal transformations on u, w, and z for practical implementation of Theorem 3 are briefly summarized.

3. Space Station Model

The robust control synthesis technique developed in Section 2 is applied to the Space Station subject to large payload operations which cause significant changes in the moments of inertia of the system. Dynamical equations of the Space Station are briefly reviewed (for details, see [3,4]).

The Space Station in a circular orbit is expected to maintain local-vertical and local-horizontal (LVLH) orientation during normal mode operation. For small attitude deviations from LVLH orientation, the linearized equations of motion can be written as:

Space Station Dynamics:

$$\begin{bmatrix} I_{11} & I_{12} & I_{13} \\ I_{21} & I_{22} & I_{23} \\ I_{31} & I_{32} & I_{33} \end{bmatrix} \begin{bmatrix} \dot{\omega}_1 \\ \dot{\omega}_2 \\ \dot{\omega}_3 \end{bmatrix} = n \begin{bmatrix} I_{31}, & 2I_{32}, & I_{33}-I_{22} \\ -I_{32}, & 0, & I_{12} \\ I_{22}-I_{11}, & -2I_{12}, & -I_{13} \end{bmatrix} \begin{bmatrix} \omega_1 \\ \omega_2 \\ \omega_3 \end{bmatrix} + 3n^2 \begin{bmatrix} I_{33}-I_{22}, & I_{21}, & 0 \\ I_{12}, & I_{33}-I_{11}, & 0 \\ -I_{13}, & -I_{23}, & 0 \end{bmatrix} \begin{bmatrix} \theta_1 \\ \theta_2 \\ \theta_3 \end{bmatrix} + n^2 \begin{bmatrix} -2I_{23} \\ 3I_{13} \\ -I_{12} \end{bmatrix} + \begin{bmatrix} -u_1+w_1 \\ -u_2+w_2 \\ -u_3+w_3 \end{bmatrix} \quad (24)$$

Attitude Kinematics:

$$\dot{\theta}_1 - n\theta_3 = \omega_1 \quad (25a)$$
$$\dot{\theta}_2 - n = \omega_2 \quad (25b)$$
$$\dot{\theta}_3 + n\theta_1 = \omega_3 \quad (25c)$$

CMG Momentum:

$$\dot{h}_1 - nh_3 = u_1 \quad (26a)$$
$$\dot{h}_2 = u_2 \quad (26b)$$
$$\dot{h}_3 + nh_1 = u_3 \quad (26c)$$

where (1, 2, 3) are the roll, pitch, and yaw control axes whose origin is fixed at the mass center, with the roll axis in the flight direction, the pitch axis perpendicular to the orbit plane, and the yaw axis toward the Earth; (θ_1, θ_2, θ_3) are the roll, pitch, yaw Euler angles of the body axes with respect to LVLH axes which rotate with the orbital angular velocity, n; ($\omega_1, \omega_2, \omega_3$) are the body-axis components of the absolute angular velocity of the station; (I_{11}, I_{22}, I_{33}) are the principal moments of inertia; I_{ij} ($i \neq j$) are the products of inertia; (h_1, h_2, h_3) are the body-axis components of the CMG momentum; (u_1, u_2, u_3) are the body-axis components of the control torque caused by CMG momentum change; (w_1, w_2, w_3) are the body-axis components of the external disturbance torque; and n is the orbital rate of 0.0011 rad/sec.

Note that the products of inertia cause three-axis coupling as well as a bias torque in each axis. Fortunately, most practical situations with small products of inertia permit further simplification in such a way that pitch motion is uncoupled from roll/yaw motion. For the case where the control axes are nearly aligned with the principal axes ($I_1 \triangleq I_{11}$, $I_2 \triangleq I_{22}$, and $I_3 \triangleq I_{33}$), Eqs. (24) become

$$\dot{\omega}_1 + nk_1\omega_3 + 3n^2k_1\theta_1 = -b_1u_1 + b_1w_1 \quad (27a)$$
$$\dot{\omega}_2 + 3n^2k_2\theta_2 = -b_2u_2 + b_2w_2 \quad (27b)$$
$$\dot{\omega}_3 - nk_3\omega_1 = -b_3u_3 + b_3w_3 \quad (27c)$$

where

$$k_1=(I_2-I_3)/I_1, \qquad b_1=1/I_1,$$
$$k_2=(I_1-I_3)/I_2, \qquad b_2=1/I_2,$$
$$k_3=(I_2-I_1)/I_3, \qquad b_3=1/I_3.$$

Inertia matrices of the Phase 1 Space Station as well as the assembly flight #3 are listed in Table 1. In this paper, only the Phase 1 configuration is considered. The uncontrolled Space Station with such inertia properties is in an unstable equilibrium when $\theta_i = 0$ ($i = 1, 2, 3$). Also included are expected aerodynamic disturbances which are modeled as bias plus cyclic terms in the body-fixed control axes:

$$w(t) = \text{Bias} + A_n \sin(nt+\phi_n) + A_{2n} \sin(2nt+\phi_{2n}) \quad (28)$$

The cyclic component at orbital rate is due to the effect of Earth's diurnal bulge, while the cyclic torque at twice the orbital rate is caused by the rotating solar panels. The magnitudes and phases of aerodynamic torque in each axis are unknown for control design.

4. Space Station Control

A robust H_∞ control design for the Space Station is described here. The Space Station is desired to have a control system which accommodates the periodic disturbances and large inertia variations. In [3,4], a periodic-disturbance accommodating controller is developed for the Space Station, and the disturbance rejection filters for the control of h_1, θ_2, θ_3 are assumed to have the following forms:

$$\ddot{\alpha}_1 + (n)^2\alpha_1 = h_1 \quad (29a)$$
$$\ddot{\beta}_1 + (2n)^2\beta_1 = h_1 \quad (29b)$$
$$\ddot{\alpha}_2 + (n)^2\alpha_2 = \theta_2 \quad (29c)$$
$$\ddot{\beta}_2 + (2n)^2\beta_2 = \theta_2 \quad (29d)$$
$$\ddot{\alpha}_3 + (n)^2\alpha_3 = \theta_3 \quad (29e)$$
$$\ddot{\beta}_3 + (2n)^2\beta_3 = \theta_3 \quad (29f)$$

The pitch control logic, involving the single control input u_2 and eight states, is then expressed as

$$u_2 = K_{22} x_2 \tag{30}$$

where K_{22} is a 1×8 gain matrix and x_2 is the state vector defined as

$$x_2 \triangleq [\theta_2\ \dot{\theta}_2\ h_2\ \int h_2\ \alpha_2\ \dot{\alpha}_2\ \beta_2\ \dot{\beta}_2]^T. \tag{31}$$

The CMG momentum and its integral are included to prevent CMG momentum build-up.

Similarly the roll/yaw control logic is given by two control inputs, u_1 and u_3, and sixteen states:

$$\begin{bmatrix} u_1 \\ u_3 \end{bmatrix} = \begin{bmatrix} K_{11} & K_{13} \\ K_{31} & K_{33} \end{bmatrix} \begin{bmatrix} x_1 \\ x_3 \end{bmatrix} \tag{32}$$

where K_{ij}'s are 1×8 gain matrices and

$$x_1 \triangleq [\theta_1\ \omega_1\ h_1\ \int h_1\ \alpha_1\ \dot{\alpha}_1\ \beta_1\ \dot{\beta}_1]^T, \tag{33a}$$

$$x_3 \triangleq [\theta_3\ \omega_3\ h_3\ \int h_3\ \alpha_3\ \dot{\alpha}_3\ \beta_3\ \dot{\beta}_3]^T. \tag{33b}$$

Directional inertia variations for the Space Station are modeled as

$$\begin{bmatrix} \Delta I_1 & \Delta I_2 & \Delta I_3 \end{bmatrix} = \delta_1 \begin{bmatrix} I_1 & 0 & I_1 \end{bmatrix} \tag{34a}$$

$$\begin{bmatrix} \Delta I_1 & \Delta I_2 & \Delta I_3 \end{bmatrix} = \delta_2 \begin{bmatrix} I_1 & I_2 & I_3 \end{bmatrix} \tag{34b}$$

$$\begin{bmatrix} \Delta I_1 & \Delta I_2 & \Delta I_3 \end{bmatrix} = \delta_3 \begin{bmatrix} I_1 & 0 & -I_3 \end{bmatrix} \tag{34c}$$

$$\begin{bmatrix} \Delta I_1 & \Delta I_2 & \Delta I_3 \end{bmatrix} = \delta_4 \begin{bmatrix} I_1 & -I_2 & 0 \end{bmatrix} \tag{34d}$$

$$\begin{bmatrix} \Delta I_1 & \Delta I_2 & \Delta I_3 \end{bmatrix} = \delta_5 \begin{bmatrix} I_1 & I_2 & -I_3 \end{bmatrix} \tag{34e}$$

where δ_i's represent the amounts of directional parameter variations with respect to the nominal inertias I_1, I_2, and I_3. The directional variation involving δ_i is called a δ_i-inertia variation in this paper. As discussed in [4], there exist physical bounds for δ_i's due to the inherent physical properties of the gravity-gradient stabilization and the moments of inertia itself. Table 2 summarizes such physical limitations on δ_i-inertia variations. As discussed in [3,4], the Phase 1 Space Station becomes unstable for as little as -7 % variation in I_3 and $+8$ % variation in I_1, because of the inherent physical nature of the problem.

The robust controller synthesis in this paper is primarily concerned with the δ_1- and δ_2-inertia variations. In particular, the δ_1-inertia variation is physically caused by the translational motion of the payload along the pitch axis, as illustrated in Fig. 1.

Pitch Control

The pitch-axis dynamics with nominal inertias are described as:

$$\frac{d}{dt}\begin{bmatrix} \theta_2 \\ \dot{\theta}_2 \end{bmatrix} = \begin{bmatrix} 0 & 1 \\ -3n^2 k_2 & 0 \end{bmatrix} \begin{bmatrix} \theta_2 \\ \dot{\theta}_2 \end{bmatrix} + \begin{bmatrix} 0 \\ b_2 \end{bmatrix} [-u_2] \tag{35}$$

where the external disturbance is not included since it is accommodated by the disturbance rejection filter.

Since the δ_1-inertia variation does not affect the pitch dynamics (i.e., k_2 and b_2 remain constant), only the δ_2-inertia variation, where only b_2 has uncertainty, is considered for the pitch axis.

An input-output decomposition of the perturbed control distribution matrix ΔB_2 in Eq. (35) is obtained as

$$\Delta B_2 = \begin{bmatrix} 0 \\ \frac{1}{I_2(1+\delta_2)} - \frac{1}{I_2} \end{bmatrix} = -\mathbf{MEN}$$

and

$$M = \begin{bmatrix} 0 \\ b_2 \end{bmatrix}, \quad E = \delta_2', \quad N = -1,$$

where $b_2 = 1/I_2$ for the nominal inertia and $\delta_2' = 1/(1+\delta_2) - 1$.

The fictitious input w_p and the fictitious output z_p for the pitch axis with the δ_2-inertia variation are then expressed as

$$z_p = N[-u_2] = u_2 \tag{36a}$$

$$w_p = -E z_p = -\delta_2' z_p \tag{36b}$$

These equations replace the parameter variations in Eq. (35) as follows:

$$\frac{d}{dt}\begin{bmatrix} \theta_2 \\ \dot{\theta}_2 \end{bmatrix} = \begin{bmatrix} 0 & 1 \\ -3n^2 k_2 & 0 \end{bmatrix} \begin{bmatrix} \theta_2 \\ \dot{\theta}_2 \end{bmatrix} + \begin{bmatrix} 0 \\ b_2 \end{bmatrix} [w_p - u_2] \tag{37a}$$

$$z_p = u_2 \tag{37b}$$

$$w_p = -\delta_2' z_p \tag{37c}$$

where $k_2 = (I_3 - I_1)/I_2$ with the nominal inertias.

The robust control problem for Eqs. (35) now becomes a disturbance attenuation problem for Eqs. (37), to which Theorems 2 and 3 can be applied. Note that z_p contains only the control input u_2. This uncertainty in the control loop introduces a necessary tradeoff between stability robustness and performance.

Equations (37) are now augmented by the pitch CMG momentum dynamics described by Eq. (26b) and disturbance rejection filters described by Eqs. (29c) and (29d). The augmented state vector is x_2 as defined in Eq. (31), and the controlled output z is also formed as

$$z = \begin{bmatrix} x_2 \\ u_2 \end{bmatrix}$$

With proper selections of the weighting factors, scaling, and orthogonal transformations, as discussed in the appendix, the augmented system equations are transformed to satisfy the assumption (ii) in Theorem 3. The performance specification bound γ is chosen to be 1, and a set of weighting factors used in this paper is summarized in Table 7.

By solving the Riccati equation, Eq. (22), a robust H_∞ full-state feedback controller for the pitch axis is obtained with a control gain matrix listed in Table 3. The closed-loop eigenvalues of the nominal system with this gain matrix are listed in Table 4. Stability margins of this new robust H_∞ controller with respect to the inertia variations are compared in Table 5 to those of the previous LQR design in [3]. A significant margin of 70% for the δ_2-inertia variation is achieved (compared to the 34% margin of the LQR design). As can be seen in Table 4, however, this new pitch controller has a closed-loop pole at $-8.38n$ which is relatively large compared to that of the conventional LQR design of Ref. 3. As discussed in [14], an H_∞ controller often achieves the desired robustness by having a high bandwidth for a single input system. The pitch axis design here is such a case; but the robust H_∞ control design for the multi-input case to be discussed in the next section has a remarkable stability robustness margin with nearly the same bandwidth as the conventional LQR design.

Figure 2 shows the time responses of the nominal closed-loop system to the initial conditions $\theta_2(0) = 1$ degree and $\dot{\theta}_2(0) = 0.001$ deg/sec, and the disturbance input w_2 in Table 1. The time responses are comparable to those of the LQR designs in [3,4].

Roll/Yaw Control

Consider the roll/yaw dynamics with nominal parameters described by

$$\begin{bmatrix} \dot{\theta}_1 \\ \dot{\omega}_1 \\ \dot{\theta}_3 \\ \dot{\omega}_3 \end{bmatrix} = \begin{bmatrix} 0 & 1 & n & 0 \\ -3n^2k_1 & 0 & 0 & -nk_1 \\ -n & 0 & 0 & 1 \\ 0 & nk_3 & 0 & 0 \end{bmatrix} \begin{bmatrix} \theta_1 \\ \omega_1 \\ \theta_3 \\ \omega_3 \end{bmatrix} + \begin{bmatrix} 0 & 0 \\ b_1 & 0 \\ 0 & 0 \\ 0 & b_3 \end{bmatrix} \begin{bmatrix} -u_1 \\ -u_3 \end{bmatrix} \tag{38}$$

where the external disturbances are not included. Variations in k_1, k_3, b_1, and b_3 caused by perturbations in the moments of inertia are approximated as follows:

$$\Delta k_1 \cong -k_1 \frac{\Delta I_1}{I_1} + \frac{\Delta I_2}{I_1} - \frac{\Delta I_3}{I_1},$$
$$\Delta k_3 \cong -\frac{\Delta I_1}{I_3} + \frac{\Delta I_2}{I_3} - k_3 \frac{\Delta I_3}{I_3},$$
$$\Delta b_1 \cong -b_1 \frac{\Delta I_1}{I_1}, \qquad \Delta b_3 \cong -b_3 \frac{\Delta I_3}{I_3},$$

where $k_1 = (I_2 - I_3)/I_1$, $k_3 = (I_2 - I_1)/I_3$, $b_1 = 1/I_1$, and $b_3 = 1/I_3$, for the nominal inertias.

In particular, for the δ_1-inertia variation, the above parameter variations become:

$$\Delta k_1 \cong -(k_1 + 1)\delta_1, \qquad \Delta b_1 \cong -b_1\delta_1,$$
$$\Delta k_3 \cong -(k_3 + 1)\frac{I_1}{I_3}\delta_1, \qquad \Delta b_3 \cong -b_3\frac{I_1}{I_3}\delta_1.$$

An input-output decomposition of the perturbed system matrix Δ_e is then obtained as:

$$\Delta_e = -\boldsymbol{M}\,\boldsymbol{E}\,[\ \boldsymbol{N}_x \quad \boldsymbol{N}_u\ ]$$

or

$$\boldsymbol{M} = \begin{bmatrix} 0 & 0 \\ b_1 & 0 \\ 0 & 0 \\ 0 & b_3 \end{bmatrix}, \qquad \boldsymbol{E} = \begin{bmatrix} \delta_1 & 0 \\ 0 & \delta_1 \end{bmatrix},$$
$$\boldsymbol{N}_x = \begin{bmatrix} -3n^2 I_a & 0 & 0 & -nI_a \\ 0 & n\frac{I_1}{I_3}I_b & 0 & 0 \end{bmatrix},$$
$$\boldsymbol{N}_u = \begin{bmatrix} -1 & 0 \\ 0 & -\frac{I_1}{I_3} \end{bmatrix},$$

where $I_a \triangleq I_2 - I_3 + I_1$ and $I_b \triangleq I_2 - I_1 + I_3$.

The fictitious input $\boldsymbol{w}_p$ and output $\boldsymbol{z}_p$ for the roll/yaw control design incorporating the δ_1-inertia variation are expressed as

$$\boldsymbol{z}_p = \boldsymbol{N}_x\boldsymbol{x} + \boldsymbol{N}_u \begin{bmatrix} -u_1 \\ -u_3 \end{bmatrix} \tag{39a}$$
$$\boldsymbol{w}_p = -\boldsymbol{E}\boldsymbol{z}_p = -\delta_1\,\boldsymbol{z}_p \tag{39b}$$

where $\boldsymbol{x} \triangleq [\theta_1\ \ \omega_1\ \ \theta_3\ \ \omega_3]^T$. The perturbed system is then expressed by the nominal system and the internal feedback loop as

$$\dot{\boldsymbol{x}} = \boldsymbol{A}\boldsymbol{x} + \boldsymbol{B}[\boldsymbol{w}_p - \boldsymbol{u}] \tag{40a}$$
$$\boldsymbol{z}_p = \boldsymbol{N}_x\boldsymbol{x} - \boldsymbol{N}_u\boldsymbol{u} \tag{40b}$$
$$\boldsymbol{w}_p = -\delta_1\,\boldsymbol{z}_p \tag{40c}$$

where $\boldsymbol{u} \triangleq [u_1\ u_3]^T$, $\boldsymbol{B} \triangleq \boldsymbol{M}$ and

$$\boldsymbol{A} \triangleq \begin{bmatrix} 0 & 1 & n & 0 \\ -3n^2k_1 & 0 & 0 & -nk_1 \\ -n & 0 & 0 & 1 \\ 0 & nk_3 & 0 & 0 \end{bmatrix}.$$

Similarly to the pitch-axis design, the standard state-space representation given by Eq. (1) can be constructed by redefining $\boldsymbol{w}$ and $\boldsymbol{z}$. A roll/yaw gain matrix of the robust H_∞ controller is listed in Table 3 for the particular weighting factors chosen as in Table 7. The closed-loop eigenvalues of the nominal system with this robust H_∞ controller are listed in Table 4. Stability margins of this new controller are compared to those of other previous designs in Table 6. Similarly to the pitch control design, the robust H_∞ controller for the coupled roll/yaw axes has significant improvement in stability margins over the standard LQR design (e.g., the 73% margin over the 44% margin for the δ_1-inertia variation). Contrary to the pitch case with a single control input, however, the robust H_∞ controller for the roll/yaw axes with two control inputs has a relatively low bandwidth! In fact, the roll/yaw closed-loop poles shown in Table 4 are very comparable to those of LQR designs in [3–5].

Figure 3 shows the time responses of the nominal closed-loop system to the initial conditions $\theta_1(0) = \theta_3(0) = 1$ deg and $\dot{\theta}_1(0) = \dot{\theta}_3(0) = 0.001$ deg/sec, and the disturbance input w_1 and w_3 in Table 1.

5. Summary

Major results and contributions of this paper are summarized in this section. A robust control synthesis technique presented in Section 2, which is primarily based on the results in [10,13] and the state-space formulation of the H_∞ control theory in [8,9], further exploits the concept of linearized, directional variations of nonlinear, structured uncertain parameters. Applications of this approach to the full-state feedback control design problem of the Space Station with uncertain inertia property have resulted in the following interesting results: (1) For the pitch control with a single input, the stability robustness improvement with respect to the overall inertia increases has been achieved mainly by having a relatively high bandwidth controller and (2) The robust H_∞ control design for the roll/yaw axis with two control inputs has achieved significant stability robustness over the LQR design, even with relatively low bandwidth. In other words, the concept of linearized directional parameter variation, combined with the standard H_∞ control theory, has been shown to be a practical way for designing parameter-insensitive controllers.

For roll/yaw control, the δ_1-inertia variation was considered in robust H_∞ control design to accommodate the moments-of-inertia variations caused by the translational motion of a large payload along the pitch axis (see Fig. 1). Since the δ_1-inertia variation does not affect the pitch dynamics, the δ_2-inertia variation was considered for the pitch control design. It is also emphasized that the closed-loop system with this new robust H_∞ controller is stable for $\pm 73\%$ δ_1-inertia variation and for $\pm 70\%$ δ_2-inertia variation, compared to the $\pm 44\%$ δ_1 and $\pm 34\%$ δ_2 stability margins of a typical LQR design.

6. Conclusions

A robust control synthesis technique for uncertain dynamical systems subject to nonlinear, structured parameter perturbations has been presented, which is based on the H_∞ control theory and the internal feedback loop modeling concept. This technique was applied to the multivariable, full-state feedback control design problem of the Space Station, resulting in remarkable stability margins with respect to the moments-of-inertia uncertainty over the conventional linear-quadratic-regulator designs. The linearized, directional parameter variation concept was shown to be a proper way of accommodating the nonlinear, structured parameter variations in the design of a parameter-insensitive controller.

Appendix

In general, the H_∞ control theory considers frequency-dependent weighting matrices for the shaping of closed-loop transfer function $\boldsymbol{T}_{zw}$. Proper selection of the weighting matrices, however, is not always obvious. One practical way is to use a constant diagonal weighting matrix and a normalized output equation. Proper scaling and orthogonal transformations can be employed to satisfy the assumptions in Theorem 3.

Consider a system given by

$$\dot{\boldsymbol{x}} = \boldsymbol{A}\boldsymbol{x} + \boldsymbol{B}_1\boldsymbol{w} + \boldsymbol{B}_2\boldsymbol{u}$$
$$\boldsymbol{z} = \begin{bmatrix} \boldsymbol{z}^{(1)} \\ \boldsymbol{z}^{(2)} \end{bmatrix} = \begin{bmatrix} \boldsymbol{C}_1^{(1)} \\ \boldsymbol{0} \end{bmatrix} \boldsymbol{x} + \begin{bmatrix} \boldsymbol{D}_{12}^{(1)} \\ \boldsymbol{D}_{12}^{(2)} \end{bmatrix} \boldsymbol{u}$$

where $\boldsymbol{D}_{12}^{(2)}$ is assumed nonsingular.

Define $\boldsymbol{r}_{z^{(1)}}$, $\boldsymbol{r}_{z^{(2)}}$, and $\boldsymbol{r}_w$ be the weighting factors with dimensions of p_1, m_2, and m_1, respectively. The weighting matrices $\boldsymbol{Q}$, $\boldsymbol{R}$, and $\boldsymbol{W}$ are then defined as:

$$\boldsymbol{Q} = [\mathrm{diag}\{\boldsymbol{r}_{z^{(1)}}\}]^{-1}$$
$$\boldsymbol{R} = [\mathrm{diag}\{\boldsymbol{r}_{z^{(2)}}\}]^{-1}$$
$$\boldsymbol{W} = [\mathrm{diag}\{\boldsymbol{r}_w\}]^{-1}$$

Define normalized variables as

$$\bar{\boldsymbol{z}}^{(1)} = \boldsymbol{Q}\boldsymbol{z}^{(1)}$$
$$\bar{\boldsymbol{z}}^{(2)} = \boldsymbol{R}\boldsymbol{z}^{(2)}$$
$$\bar{\boldsymbol{w}} = \boldsymbol{W}\boldsymbol{w}$$

A scaling factor $\boldsymbol{S}$ for $\boldsymbol{u}$ is also defined as:

$$\bar{\boldsymbol{u}} = \boldsymbol{S}\boldsymbol{u}$$

Substituting the above new variables into the system equation gives

$$\dot{\boldsymbol{x}} = \boldsymbol{A}\boldsymbol{x} + \boldsymbol{B}_1\boldsymbol{W}^{-1}\bar{\boldsymbol{w}} + \boldsymbol{B}_2\boldsymbol{S}^{-1}\bar{\boldsymbol{u}}$$
$$\begin{bmatrix} \boldsymbol{Q}^{-1}\bar{\boldsymbol{z}}^{(1)} \\ \boldsymbol{R}^{-1}\bar{\boldsymbol{z}}^{(2)} \end{bmatrix} = \begin{bmatrix} \boldsymbol{C}_1^{(1)} \\ \boldsymbol{0} \end{bmatrix} \boldsymbol{x} + \begin{bmatrix} \boldsymbol{D}_{12}^{(1)} \\ \boldsymbol{D}_{12}^{(2)} \end{bmatrix} \boldsymbol{S}^{-1}\bar{\boldsymbol{u}}$$

The controlled output equation can be rewritten as

$$\begin{bmatrix} \bar{\boldsymbol{z}}^{(1)} \\ \bar{\boldsymbol{z}}^{(2)} \end{bmatrix} = \begin{bmatrix} \boldsymbol{Q}\boldsymbol{C}_1^{(1)} \\ \boldsymbol{0} \end{bmatrix} \boldsymbol{x} + \begin{bmatrix} \boldsymbol{Q}\boldsymbol{D}_{12}^{(1)} \\ \boldsymbol{R}\boldsymbol{D}_{12}^{(2)} \end{bmatrix} \boldsymbol{S}^{-1}\bar{\boldsymbol{u}}$$

with a QR decomposition of the matrix

$$\begin{bmatrix} \boldsymbol{Q}\boldsymbol{D}_{12}^{(1)} \\ \boldsymbol{R}\boldsymbol{D}_{12}^{(2)} \end{bmatrix} = \boldsymbol{P} \begin{bmatrix} \boldsymbol{0} \\ \boldsymbol{L} \end{bmatrix}$$

where $\boldsymbol{P}$ is an orthogonal transformation matrix and $\boldsymbol{L}$ is lower-triangular (or generally nonsingular).

If the control scaling matrix $\boldsymbol{S}$ can be defined as

$$\boldsymbol{S} = \boldsymbol{L}^{-1}$$

the following system equation then satisfies the assumptions (ii) and (iv) in Theorem 3:

$$\begin{aligned} \dot{x} &= Ax + B_1 W^{-1}\bar{w} + B_2 L\bar{u} \\ P^T \begin{bmatrix} \bar{z}^{(1)} \\ \bar{z}^{(2)} \end{bmatrix} &= P^T \begin{bmatrix} QC_1^{(1)} \\ 0 \end{bmatrix} x + \begin{bmatrix} 0 \\ I \end{bmatrix} \bar{u} \end{aligned}$$

where P^T does not affect the H_∞ norm property.

The system matrices are redefined, to be implemented in a computer software (e.g., CTRL-C), as

$$B_1 \leftarrow B_1 W^{-1}, \qquad B_2 \leftarrow B_2 L,$$
$$C_1 \leftarrow P^T \begin{bmatrix} QC_1^{(1)} \\ 0 \end{bmatrix}, \qquad D_{12} \leftarrow \begin{bmatrix} 0 \\ I \end{bmatrix}.$$

Finally the actual control gain matrix K is obtained by re-scaling the normalized gain matrix $\bar{K}$ as:

$$K = S^{-1}\bar{K}$$

The weighting factors selected for the example design of this paper are listed in Table 7.

References

[1] J.A. Yeichner, J.F. Lee, and D. Barrows, "Overview of Space Station Attitude Control System with Active Momentum Management," AAS Paper No. 88-044, 11th Annual AAS Guidance and Control Conference, 1988.

[2] H.H. Woo, H.D. Morgan, and E.T. Falangas, "Momentum Management and Attitude Control Design for a Space Station," *Journal of Guidance, Control, and Dynamics*, Vol. 11, No. 1, pp. 19-25, Jan.-Feb., 1988.

[3] B. Wie, K.W. Byun, V.W. Warren, D. Geller, D. Long, and J. Sunkel, "New Approach to Attitude/Momentum Control of the Space Station," *Journal of Guidance, Control, and Dynamics*, Vol. 12, No. 5, pp. 714-722, Sept.-Oct., 1989.

[4] V.W. Warren, B. Wie, and D. Geller, "Periodic-Disturbance Accommodating Control of the Space Station," AIAA Paper No. 89-3476, to appear in the *Journal of Guidance, Control, and Dynamics.*

[5] J.T. Harduvell, "Comparison of Continuous Momentum Control Approaches for the Space Station," Internal Memo A95-J845-JTH-M-8802099, Space Station Division, McDonnell Douglas Astronautics Co., Sept. 26, 1989.

[6] J. Sunkel and L.S. Shieh, "An Optimal Momentum Management Controller for the Space Station," AIAA Paper No. 89-3474, to appear in the *Journal of Guidance, Control, and Dynamics.*

[7] B. Wie, A. Hu, and R. Singh, "Multi-Body Interaction Effects on Space Station Attitude Control and Momentum Management," AIAA Paper No. 89-3514, to appear in the *Journal of Guidance, Control, and Dynamics.*

[8] J. Doyle, K. Glover, P. Khargonekar, and B. Francis, "State-Space Solutions to Standard H_2 and H_∞ Control Problems," *IEEE Transactions on Automatic Control*, Vol. 34, No. 8, pp. 831-847, Aug., 1989.

[9] K. Glover and J. Doyle, "State-Space Formulae for All Stabilizing Controllers that Satisfy an H_∞-norm Bound and Relations to Risk Sensitivity," *Systems & Control Letters*, No.11, pp. 167-172, 1988.

[10] K.W. Byun, *Robust Controller Synthesis for Uncertain Dynamical Systems*, Ph.D. Dissertation, Dept. of Aerospace Engineering and Engineering Mechanics, The University of Texas at Austin, May 1990.

[11] B.G. Morton and R.M. McAfoos, "A Mu-Test for Robustness Analysis of a Real-Parameter Variation Problem," *Proc. of ACC*, pp. 135-138, June, 1985.

[12] M. Tahk and J.L. Speyer, "Modeling of Parameter Variations and Asymptotic LQG Synthesis," *IEEE Transactions on Automatic Control*, Vol. AC-32, No. 9, pp. 793-801, Sept., 1987.

[13] K.W. Byun, B. Wie, and J. Sunkel, "Robust Control Synthesis for Uncertain Dynamical Systems," AIAA Paper No. 89-3516, submitted to the *Journal of Guidance, Control, and Dynamics.*

[14] A.E. Bryson, Jr. and A. Carrier, "A Comparison of Control Synthesis Using Differential Games (H-infinity) and LQR," AIAA Paper No. 89-3598.

[15] B.A. Francis, *A Course in H_∞ Control Theory*, Springer-Verlag Berlin, Heidelberg, 1987.

[16] E. Wedell, C.-H. Chuang, and B. Wie, "Computational Analysis of a Stability Robustness Margin for Structured Real-Parameter Perturbations," AIAA Paper No. 89-3504, to appear in the *Journal of Guidance, Control, and Dynamics.*

Table 1: Space Station Parameters

Parameters	Assembly Flight#3	Phase 1
Inertia (slug-ft^2)		
I_{11}	23.22E6	50.28E6
I_{22}	1.30E6	10.80E6
I_{33}	23.23E6	58.57E6
I_{12}	−0.023E6	−0.39E6
I_{13}	0.477E6	0.16E6
I_{23}	−0.011E6	0.16E6
Aerodynamic torque (ft-lb) for Phase 1		
w_1	$1+\sin(nt)+0.5\sin(2nt)$	
w_2	$4+2\sin(nt)+0.5\sin(2nt)$	
w_3	$1+\sin(nt)+0.5\sin(2nt)$	

Table 2: Physical bounds for δ_i-inertia variations

Variation Type	Lower Bound	Upper Bound
δ_1	−78.5 %‡	∞
δ_2	−100.0 %*	∞
δ_3	−2.3 %*	+7.6 %†
δ_4	−64.6 %‡	+16.4 %†
δ_5	−2.1 %*	+7.6 %†

†due to pitch open-loop characteristic.
‡due to roll/yaw open-loop characteristic.
*due to triangle inequalities for the moments of inertia.

Table 3: Robust H_∞ controller gains for the Phase 1 Space Station

Pitch K_{22}^T	Roll/Yaw K^T		Units
	6.885E+2	2.559E+2	ft-lb/rad
	4.092E+5	1.448E+5	ft-lb-sec/rad
	2.648E−3	1.495E−3	ft-lb/ft-lb-sec
	−5.563E−7	4.948E−7	ft-lb/ft-lb-sec^2
	−1.147E−10	−4.142E−10	ft-lb-rad^2/ft-lb-sec^3
	5.193E−7	2.263E−7	ft-lb-rad^2/ft-lb-sec^2
	−9.374E−10	−9.864E−10	ft-lb-rad^2/ft-lb-sec^3
	−3.783E−7	−3.204E−7	ft-lb-rad^2/ft-lb-sec^2
4.531E+2	1.800E+2	4.115E+2	ft-lb/rad
2.607E+5	8.914E+4	3.719E+5	ft-lb-sec/rad
1.169E−2	5.124E−4	2.015E−3	ft-lb/ft-lb-sec
4.518E−6	−3.149E−7	−1.997E−7	ft-lb/ft-lb-sec^2
5.673E−5	−1.567E−5	−8.042E−5	ft-lb-rad/sec^2
3.598E−2	−6.513E−2	−2.127E−3	ft-lb-rad/sec
−1.722E−5	1.892E−4	−2.489E−4	ft-lb-rad/sec^2
6.626E−2	8.709E−4	2.506E−2	ft-lb-rad/sec

Table 4: Closed-loop eigenvalues of the Phase 1 Space Station with robust H_∞ controller, in units of orbital rate, $n = 0.0011$ rad/sec

	Momentum/ Attitude	Disturbance Filter
Pitch	$-0.54 \pm 0.54j$	$-0.10 \pm 1.05j$
	$-1.53,\ -8.29$	$-0.10 \pm 2.03j$
Roll/Yaw	$-0.20,\ -0.21$	$-0.13 \pm 1.01j$
	$-0.31 \pm 0.87j$	$-0.33 \pm 1.18j$
	$-0.82 \pm 0.85j$	$-0.10 \pm 1.99j$
	$-2.31 \pm 0.65j$	$-0.27 \pm 2.06j$

Table 5: Pitch-axis stability robustness comparison

	LQR		Robust H_∞	
%	$\underline{\delta}$	$\bar{\delta}$	$\underline{\delta}$	$\bar{\delta}$
δ_1	−99	∞	−99	∞
δ_2	−89	34	−99	70
δ_3	−17	7	−27	7
δ_4	−19	16	−40	16
δ_5	−30	7	−31	7

*$\underline{\delta}$ and $\bar{\delta}$ are lower and upper bounds, respectively.

Table 6: Roll/yaw stability robustness comparison

	LQR		Local†		Robust H_∞	
%	$\underline{\delta}$	$\bar{\delta}$	$\underline{\delta}$	$\bar{\delta}$	$\underline{\delta}$	$\bar{\delta}$
δ_1	−78	44	−64	29	−78	73
δ_2	−99	43	−67	30	−99	71
δ_3	−61	80	−60	61	−58	77
δ_4	−64	64	−64	35	−64	99
δ_5	−51	68	−48	50	−49	66

†local feedback control (decentralized control).
*$\underline{\delta}$ and $\bar{\delta}$ are lower and upper bounds, respectively.

Table 7: Weighting factors used in the example design

Weightings	Pitch	Roll	Yaw	Units
θ	1.5	1.7E−3	2.1E−3	rad
$\dot{\theta}/\omega$	3.8E−3	6.1E−7	7.0E−7	rad/sec
h	8.7E+3	1.7E+4	3.0E+4	ft-lb-sec
$\int h$	3.7E+4	1.2E+5	1.8E+5	ft-lb-sec^2
α	3.5E+4	1.6E+8*	9.2E+2	sec^2/rad
$\dot{\alpha}$	2.1	1.7E+5*	8.0E−1	sec/rad
β	2.5E+4	3.7E+7*	1.5E+3	sec^2/rad
$\dot{\beta}$	1.0	3.7E+5*	3.5E−1	sec/rad
u	2.7E−2	1.0E−1	1.2E−1	ft-lb
z_p	2.7E−2	5.0E−2	5.0E−2	ft-lb
w_p	1.0E−2	1.0E−2	1.0E−2	ft-lb

*in units of ft-lb-sec^3/rad^2, ft-lb-sec^2/rad^2, ft-lb-sec^3/rad^2, and ft-lb-sec^2/rad^2, respectively.

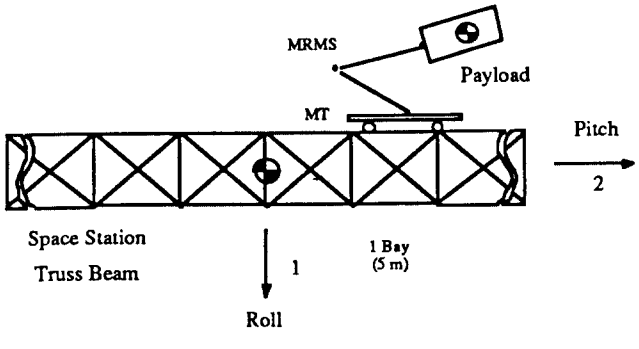

Figure 1: Space Station with MT/MRMS and its large payload.

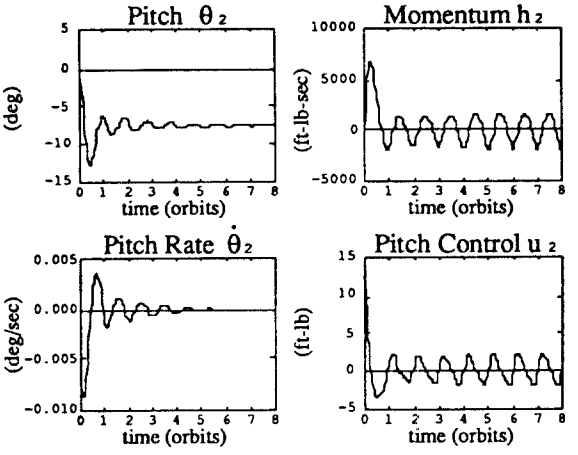

Figure 2: Pitch responses of the robust H_∞ controller.

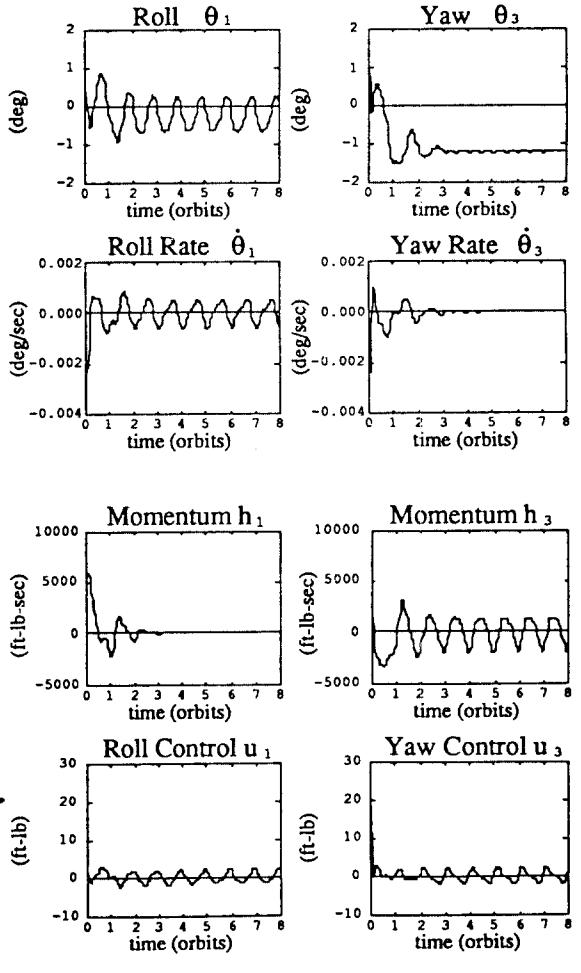

Figure 3: Roll/yaw responses of the robust H_∞ controller.